High-Performance Robotic Muscles from Conductive Nylon Sewing Thread

Michael C. Yip and Günter Niemeyer, *Member, IEEE*

***Abstract*— Natural muscles exhibit high power-to-weight ratios, inherent compliance and damping, fast actuation and high dynamic ranges. Unfortunately, traditional robotic actuators have been unable to attain similar properties, especially in a slender muscle-like form factor. Recently, super-coiled polymer (SCP) actuators have rejuvenated the promise of an artificial muscle. Constructed from commercial nylon fishing line or sewing thread and twisted until coils form, these lightweight actuators have been shown to produce significant mechanical power when thermally cycled. In this paper, we develop a thermomechanical and thermoelectric model of SCP actuators, and examine their controllability. With off-the-shelf conductive sewing thread, we show the ability to produce controlled forces in under 30 ms, exceeding human muscle performance. Finally, we use SCP actuators in a robotic hand to demonstrate their applicability as a low-cost, high performance robotic muscle.**

I. Introduction

Biological muscles have many desirable properties that make them uniquely capable actuators: (i) they are capable of a large range of forces and strains, (ii) they are inherent compliance and damping, (iii) they exhibit fast actuation times, and (iv) they have high power-to-weight ratios [1]. In addition, they are lightweight and slender. This combination of properties is unmatched by conventional robot actuator built with electric motors or pneumatic/hydraulic transmissions, and even by specialty systems as series-elastic [2] and mckibbon actuators [3].

Artificial muscle research has tried to overcome this gap. Recently, "super-coiled" polymer (SCP) actuators were shown to provide significant mechanical power in a muscle-like form factor [4]. Constructed from nylon fishing lines or sewing threads, twisted to form coils, these actuators respond to heating and cooling with contraction and relaxation.

In this paper, we examine their controllability and develop them into a high-performance muscle applicable to robotics. We use low-cost conductive sewing thread (Figure 1a,b) and apply electric current for heating. We characterize the thermo-mechanical and theromo-electric dynamics, and use the resultant models in open-loop and closed-loop control strategies. We are able to increase their dynamic performance to produce controlled forces in under 30 ms and demonstrate position tracking. Finally, we present a robot hand design utilizing SCP actuation, pictured in Figure 1c.

Michael C. Yip is with the Department of Bioengineering, Stanford University, Stanford, CA, 94305 USA. (e-mail: mcyip@stanford.edu)

Günter Niemeyer is with Disney Research, Walt Disney Imagineering, Glendale, CA, 91201 USA. (e-mail: gunter.niemeyer@disneyresearch.com)

Manuscript received Sept 30, 2014.

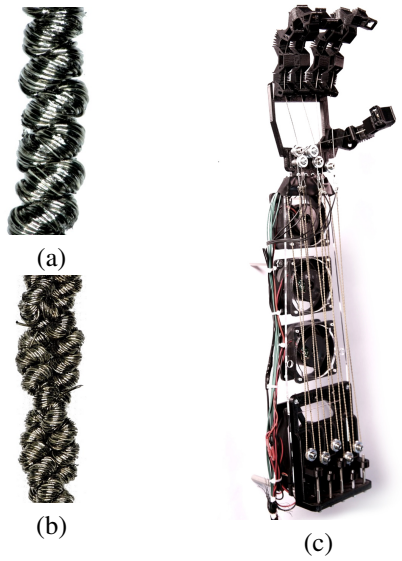

Fig. 1. (a) A conductive sewing thread is twisted until it forms coils; heat treating of the coiled thread results in an actuator that presents remarkable force and strain capabilities. These actuators can then be used for robotic applications. (b) A two-ply of the SCP actuator, comprising a pair of coiled 820um diameter coils. (c) A dexterous robotic hand constructed from SCP actuators that is light and extremely cost-effective.

II. Background

Artificial muscle research aims to create an actuator that exhibits all the desirable properties of natural muscles in a muscle-like form factor [5]. Technologies include shape memory-based alloy (SMA) actuators and shape memory polymer (SMP) actuators [6]–[10]. These materials contract and expand in their cross-section using either electrical, light, or chemical activation. Because these materials often exhibit small-strain deformations, large-scale deformation is usually achieved via parallel-plate designs [10]–[12]. Larger strains have been achieved using stacking designs [13]–[16] but these also present a more bulky actuator. The robotics community has used SMA/SMP technologies for many specialized applications [17]–[20].

It was recently discovered that by continually twisting polymer threads to an extreme until they form coils, an artificial muscle is achieved with a power-per-weight, strain, and deformation rivaling or even exceeding that of human skeletal muscle, whilst keeping a rope-like form factor [21]. These "super-coiled polymer" (SCP) actuators constructed from carbon nanotubes were capable of producing large power-to-weight ratios with repeatable contractions of up to 8% strain. Haines et al. [4] showed that the same effect

can be achieved by twisting commercially-available fishing lines and sewing threads, thus presenting an opportunity for an extremely low-cost, easily-sourced artificial muscle. In this paper, we follow their construction approach using conductive nylon sewing thread for Joule heating [22].

Our SCP actuators are composed of conductive Nylon 6,6 sewing thread. The conductive coating allows for electric heating. Multiple conductive nylon threads were tried, and the Shieldex Conductive Yarn (117/17, Denier: 240/34f, weight: 0.238g/m, coil diameter: 720um) was found to be the best in terms of strain and force production. To construct a SCP actuator, a length of the conductive thread is twisted with a motor while a 50g weight hangs off the end to keep the thread taut. As twists are inserted into the thread, the thread shortens; beyond a critical number of twists, coils begin to form along the twisted thread. When the thread is fully coiled, a voltage potential is applied across the thread and adjusted to supply approximately 0.2 W/cm length, which heats the coils to above 150°C. This heat-treatment causes the resting length of the coiled thread to plastically elongate and the coils to set. This heating cycle is undergone 20 times until the resting length converges. At this point, applying voltages to this newly-constructed SCP actuator will cause the actuator to contract. Maximum contraction for the 117/17 condutive thread used was approximately 10% before the thread burned out. In order to prevent the SCP actuators from untwisting, 2-plys were formed (Figure 1b) from single-ply coiled threads (Figure 1a). The resultant rest length at ambient temperatures $T_{amb} = 25°$ was 100 mm.

III. System Identification and Modeling

A. Experimental Apparatus

To characterize the SCP actuator, a servo-controlled tensile/strain testbed was developed. One end of an SCP actuator is attached to the testbed base, while the opposite end is attached to a load cell (LSP-2, 0-2N range, Transducer Techniques). The load cell is mounted on a vertical motion stage that is controlled by a DC servomotor, with a vertical resolution of 0.01 mm. Electrical leads at the base and at the load cell provide the voltage potential across the SCP actuator.

To quantify the thermal model aspects, the temperature of the SCP actuator must be measured and controlled. For more reliable identification, electric heating is replaced by a water tank that accommodates the the tensile testbed and the SCP actuator is used. The temperature of the water is then controlled such that the SCP actuator's temperature is known. A thermocouple (DRF-TC, Omega) is used to measure and monitor the water temperature.

B. Thermo-mechanical model

To identify the relationship between temperature, force, and strain, we elongated and relaxed the SCP actuator at different temperatures, where the temperature of the coil was set within a temperature-controlled water tank. The tension of the SCP actuator was varied between within 100 mN and 1000 mN using the servo-controlled motion stage.

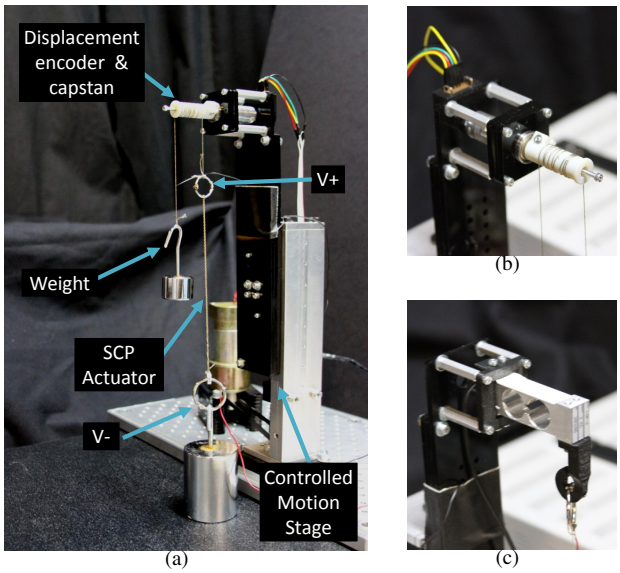

Fig. 2. (a) The experimental setup comprises a coil that is attached to a cable that wraps around a capstan, which measures the displacement/strain of the actuator under isotonic tension(b). A second attachment measures forces given isometric tension (c), where the motion stage can adjust the static strain level. The temperature of the coil is controlled using a water bath (water-filled graduated cylinder, not shown), which ensures even heat distribution, and is measured using a thermocouple placed in the water.

Figure 3a shows the force-strain profile for an SCP actuator. The profile at each temperature can be seen to shift left with increasing temperature, indicating that increasing temperature resulted in increasing force. The force shape profile is relatively constant across all temperatures. Therefore, the temperature effect on the force and strain of the SCP actuator can be considered to be independently controlled without affecting the underlying mechanical model of the actuator. The temperature effect is found to be linear with a thermal constant $c = 2.31 \pm 0.41$ mN/°C.

The underlying mechanical force-strain profile, shown in detail in Figure 3b, is a classical hysteretic behavior that can be well represented by the Preisach model. For the purposes of dynamic control of an SCP actuator, the hysteric behavior can be roughly modeled as a linear system comprising a spring and damper:

$$F = k(x - x_0) + b\dot{x}. \tag{1}$$

where k, b are the mean spring stiffness and damping of the SCP actuator. The spring stiffness is the least-squares fit to the hysteretic force-strain profile, and is found to be $k = 160 \pm 35$ N/m (6 trials). The damping parameter b is found by attaching a 50g weight to the end of an SCP actuator, allowing it to drop from a prescribed height, and then fitting (1) to the damped response (Figure 4). The damping coefficient was found to be $b = 0.84 \pm 0.12$ N/m·s (6 trials).

Combining the thermal constant with the mechanics model, we arrive at the resultant thermo-mechanical model of an SCP actuator (Figure 5):

$$F = k(x - x_0) + b\dot{x} + c(T - T_0). \tag{2}$$

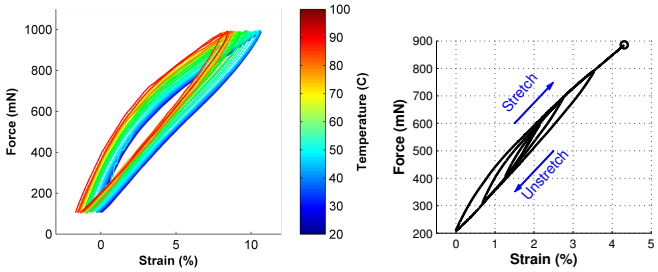

(a) (b)

Fig. 3. A force-strain profile of SCP actuators at different temperatures (a). While the force-strain curve shifts at different temperatures, the shape profile remains constant. This profile is shown in (b), which represents a classic hysteretic behavior.

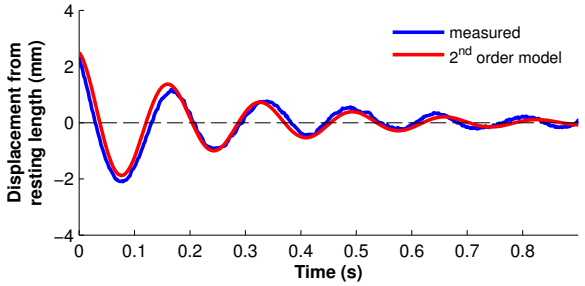

Fig. 4. A sample dynamic response of an SCP actuator, where a mass is attached to one end of the actuator and is dropped. A mass-spring-damper model, fit experimentally to the measured dynamic responses, presents a linear approximation of the mechanics of the SCP actuator.

In the following, the temperature is a controlled using current, which provides Joule heating to the actuator.

C. Thermoelectric model

The SCP actuator comprises nylon threads that are plated with silver deposits that cause it to conduct. This results in non-negligible resistance across the length of an SCP actuator, which was measured to be $R = 25\Omega$ (0.25 ± 0.005 Ω per mm). When a large enough voltage potential V is applied across the SCP actuator, the power is lost as Joule heat, $P = V^2/R$, that raises the temperature of the coils.

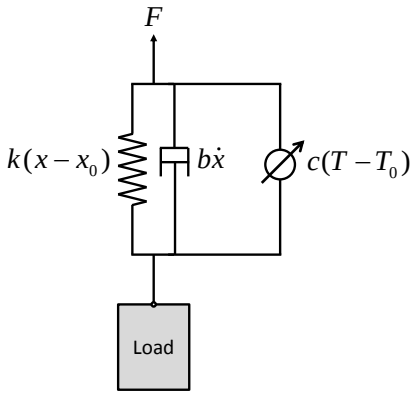

Fig. 5. The approximate model of an SCP actuator.

Because temperature was previously found to linearly correlate to force, we utilize measured force as a measurement of temperature.

A simple thermo-electrical model for an SCP actuator is

$$C_{th}\frac{dT(t)}{dt} = P(t) - \lambda(T(t) - T_{amb}) \tag{3}$$

where C_{th} is the thermal mass of the SCP actuator, $P(t)$ is the Joule heating that is applied to the SCP actuator, λ is the absolute thermal conductivity of the SCP actuator in its ambient environment, and T_{amb} is the ambient environment temperature. The absolute thermal conductivity will change depending on the environment the actuator is operating in.

Three environments are tested to investigate the heating and cooling dynamics of the SCP actuator: standing air, standing water, and forced air (168 cfm). The SCP actuators were held at a strain that resulted in a minimum tension. A step voltage was applied to the actuators, and the rise in tension was measured using a load cell. Figure 6 presents the rising and falling force profiles of the SCP actuator in (a) standing air, (b) standing water, and (c) forced air. The steady-state force and the rise-times were measured for different input voltage levels. The experiments were carried out with an ambient temperature at $T_{amb} = 25°$C. At steady-state force, $dT/dt = 0$, and the absolute thermal conductivity λ can be found (Figure 6d), where the coil temperature is found using thermal constant c from III-B. Then, given a measured rise-time and fall-time τ of the force profile given a step voltage input, the thermal mass can be found as

$$C_{th} = \tau\lambda \tag{4}$$

where the thermoelectric model is then described by the transfer function

$$\frac{T(s)}{P(s)} = \frac{1}{C_{th}s + \lambda}. \tag{5}$$

Given a step voltage input V_{ss}, the temperature response is

$$T(t) = T_{amb} + \frac{V_{ss}^2}{\lambda R}\left(1 - e^{\frac{\lambda}{C_{th}}t}\right) \tag{6}$$

Among the different environments, the absolute thermal conductivity λ of the thermo-electric model is lowest in standing air and highest in standing water. Therefore, more power is required to raise the temperature of the SCP actuator in water than the other environments, making it the least power efficient. For time constants, standing air shows the slowest rise and fall in temperature ($\tau \approx 3$ s), while forced air provides comparable thermal rise and fall times as standing water ($\tau \approx 1$ s). Since surrounding the SCP actuators in water or any other fluid in practice would result in significant increases in inertia, we therefore identified that forced air is the best environment of the three tested for getting the fastest actuation. Increasing airflow or decreasing the airflow temperature below the actuators' operating temperature will further improve the dynamic response of the actuators.

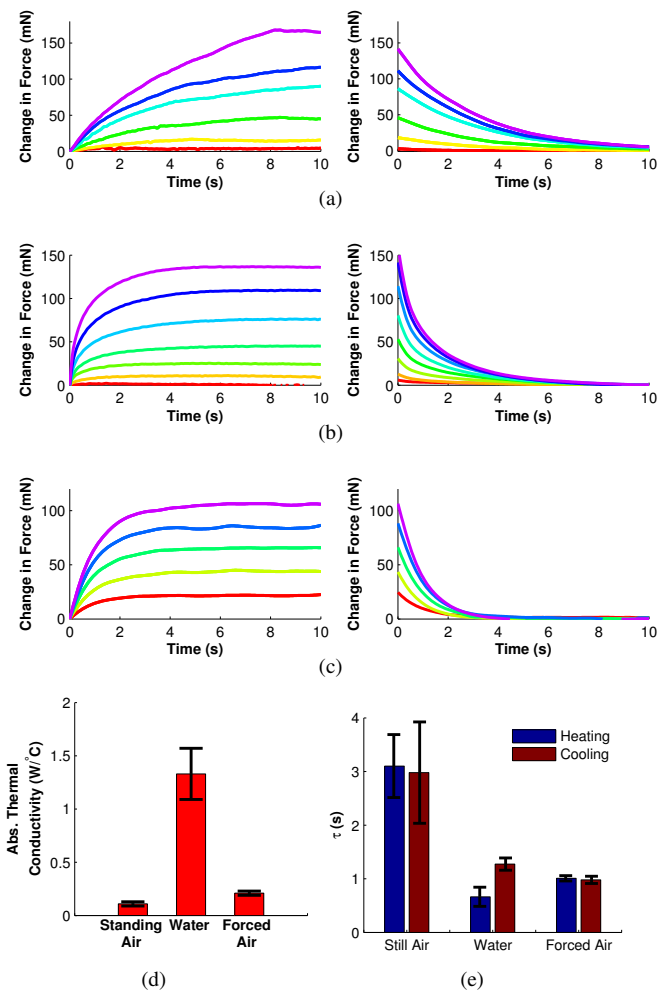

Fig. 6. Different steady state voltages (varied amongst trials) were applied across the SCP actuator to produce a range of tensions. In standing air (a), the tension rises slowly. Water (b) the tension rises quickly due to a high absolute thermal conductivity, and forced air (c) falls between the two other mediums. (d) shows the absolute thermal conductivity relating steady state temperature and electrical power, and (e) shows the rise-times and fall-times of the actuator in different environments.

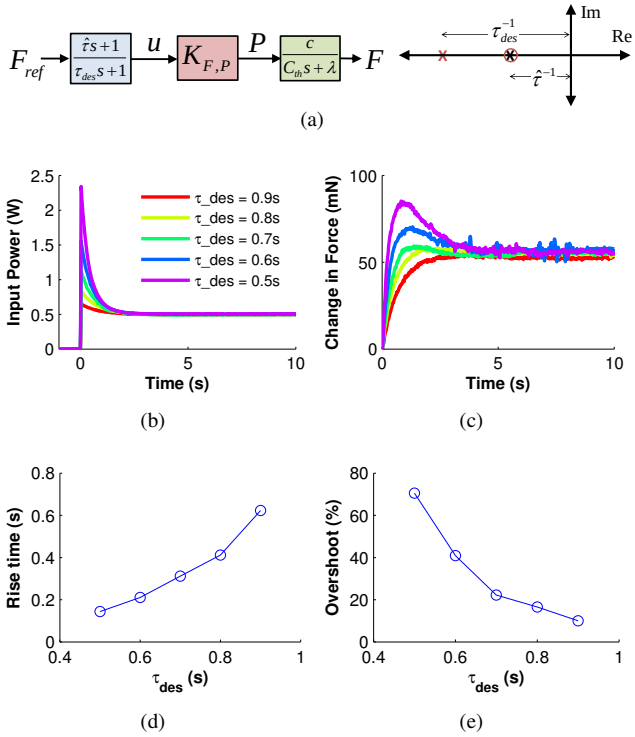

Fig. 7. (a) A lead compensator controller for the SCP actuator in isometric tension, where the pole of the actuator transfer function is cancelled out by the compensator. The input power (b) spikes to cause the temperature of the actuator to increase more quickly at the beginning, resulting in a faster change in force (c). Rise times (d) decrease with a smaller τ_{des} but overshoot(e) increases.

IV. Control Strategies

In the following section, we aim to improve the actuator's performance by using open-loop and closed-loop control to increase the speed of force accumulation. Forced air was used for all the following experiments.

A. Open-loop force control using a lead compensator

We investigated a lead compensator for an SCP actuator held in isometric tension (Figure 7). The compensator

$$\frac{\hat{\tau}s+1}{\tau_{des}s+1} \tag{7}$$

replaces the pole of the first-order thermo-mechanical model of the actuator (Figure 7a), where $\hat{\tau}$ is the estimated time constant of the actuator defined by (4) and τ_{des} is the desired time constant. The control gain $K_{F,P}$ is defined as λ/c. For a step input in the reference force, $F_{ref} = 50mN$, the input power P to the coil spikes to cause the actuator to heat more rapidly (Figure 7b,c). The power was created by applying the voltage $V = \sqrt{PR}$. Lowering the desired time constant below $\tau = 0.7s$, we observed noticeable overshoot in the system (Figure 7d,e), indicating an imperfect pole cancellation and highlighting the limits of open-loop operation.

B. Closed-loop force control

Closed-loop control (Figure 8a) can improve the speed and accuracy of force production. With a first order dynamic approximation, the root locus shows that the response of the system can theoretically be arbitrarily set (Figure 8b). Thus, with an increase in proportional gain K_p, we see significant spikes in the input power, up to 20W, but a significantly decreased response time for reaching a steady state force (Figure 8c,d). Five force levels (20, 40, 60, 80, 100 mN) were tracked. At $K_p = 50$, a response time of 28 ms was achieved on average for all reference forces, with a steady state error between $1-2\%$.

C. Position control

A more common scenario for closed-loop control of a robotic system is one that regulates the position of a mass (a robot arm and/or an object) with a position feedback sensor. We investigated the use of an SCP actuator to move and control the position of a load. A 100 g weight was attached to one end of the SCP actuator through a steel cable

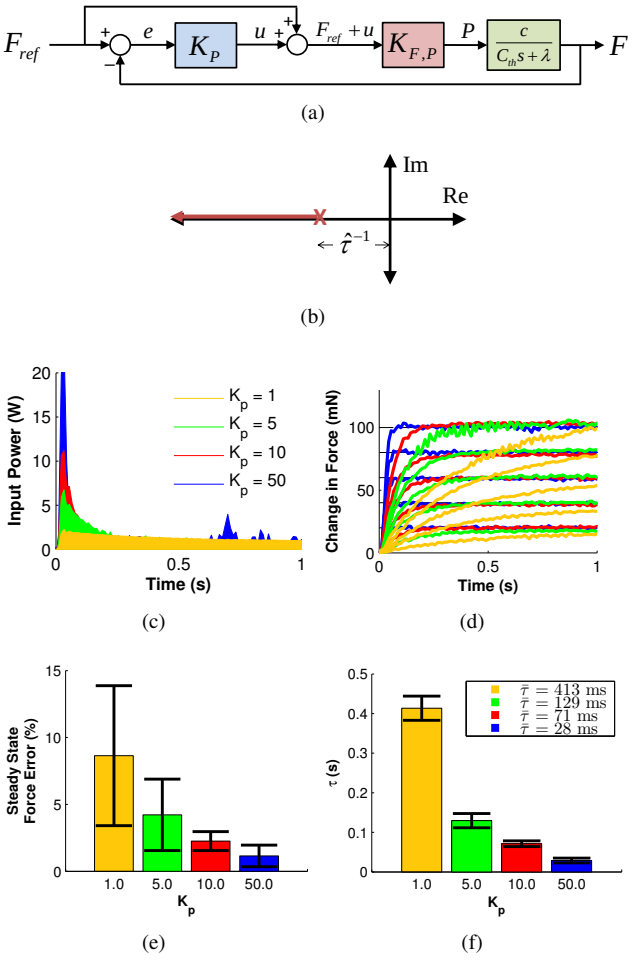

Fig. 8. (a) A closed-loop controller with a feed-forward term for the SCP actuator in isometric tension. (b) shows the input power given different proportional gains (K_p), and (c) shows the increased responsiveness of the actuator. The steady state error in applied force decreases (e) and the rise-time is lowered to 28 ms with a $K_p = 50$ (f), which is well within and exceeds the response of natural muscles.

that was wrapped around a capstan. The capstan rotation was measured using an optical encoder, which allowed the displacement of the mass to be measured at a resolution of 8 um.

The closed-loop position controller is shown in Figure 9a where, with the hanging weight, the system is represented as the standard mass-spring-damper system. The steady-state gain between displacement and input power $K_{x,P}$ was found experimentally. A proportional-derivative controller was used in conjunction with a feed-forward term to regulate the position of the mass, where $K_p = 8$, $K_d = 0.2$. The weight followed two trajectories (Figure 9b,c), one that follows a 0.1Hz sinusoidal signal, and another that was a composition of oscillating signals (0.1-0.15Hz), showing that the weight is able to track the positions accurately.

V. Robotic Muscle Demonstration

A robotic hand (Figure 10a) was constructed from 3D printed ABS material, where four fingers and a thumb, constructed as a flexure design with conduits for a tendon,

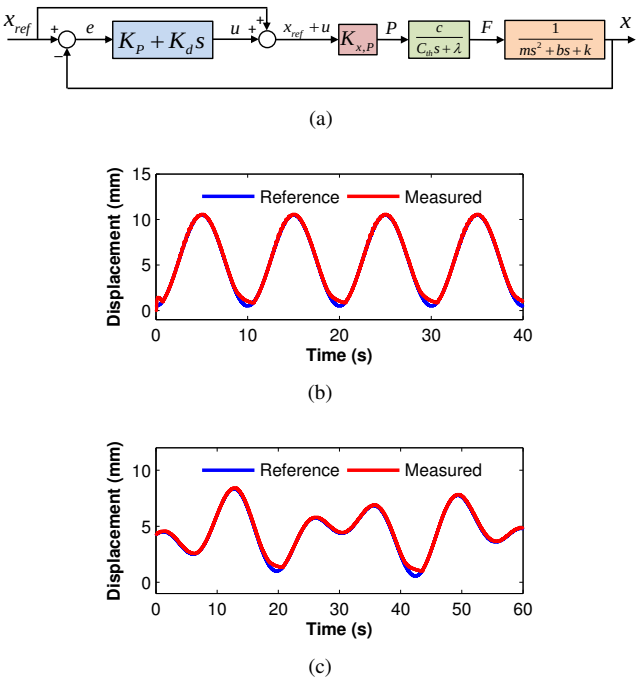

Fig. 9. The position of a weight that is attached to the end of an SCP actuator is controlled in closed-loop control (a). In (b), the position of the weight tracks a sinusoidal trajectory, while (c) tracks a more complex signal.

were actuated using one SCP actuator on each tendon. The actuators provided approximately 10-15 mm strain to cause full range of motion (fully extended digits to fist), and open-loop position control was used. The muscles were strewn along the forearm of the robot, mimicking the physical locations of the muscles in a human arm. Four small computer fans are used to cool the actuators during relaxation.

The robot arm was able to perform various grasping maneuvers, shown in (Figure 10b). The grasps were performed in under a second without the benefit of any feedback sensor, using a lead compensator to improve the speed of finger motions. Each finger can be manipulated individually, and there was no noticeable crosstalk between actuators (from convective heating, etc.).

This robot hand demonstrates that a fully articulated, five digit robot hand can be constructed using extremely inexpensive and easily-sourced materials. The hand was constructed using a Makerbot Replicator2, the drive-electronics were simple MOSFET PWM-switching supplies driven by a lab power supply, and the PWM generator was an Arduino Nano V3.0. Thus, the cost of the entire arm was less than 20 dollars.

VI. Discussion and Conclusion

In this paper, we investigated a novel robotic muscle actuator constructed from conductive sewing thread. The super-coiled sewing thread provides large actuation strains and forces per weight, is capable of responding within 30 ms to produce force when tracking a force trajectory. Position tracking has been demonstrated for a large weight, and the

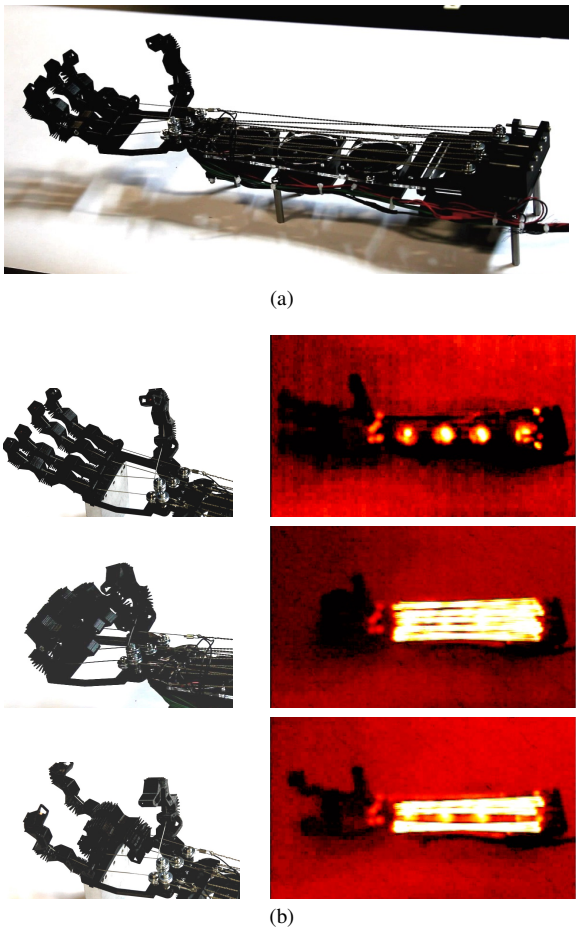

Fig. 10. A robot hand was constructed with SCP actuators for each finger (a). The hand is able to perform various grasping maneuvers (b) using open-loop control. A thermal camera provides a view of the SCP actuator heat during the grasps.

SCP actuators have been used to actuate a low-cost robotic hand.

We note the average human skeletal muscle has a twitch cycle of over 100 ms, and reaches a steady-state force in hundreds of milliseconds [23]. Furthermore, the peak power-to-weight ratio of mammalian skeletal muscle is 0.32kW/kg [1], whereas these actuators have been shown to generate up to 5.3kW/kg [4]. Using the control strategies demonstrated in this paper, we have been able to achieve performance from these SCP actuators that far exceed the speed and power of biological muscles.

In designing an SCP actuator for a specific application, we found that the choice of conductive thread alters the force and strain capabilities of the actuator. Thus, there is still a great opportunity in designing the thread material composition to optimize the actuator efficiency, range of strain, and the range of forces that can be applied. An aftermath method to improve performance of the actuator is to increase the speed of cooling of the coils during relaxation; this can be done by increasing airflow, decreasing the airflow temperature below operating temperatures, and using different gases or liquids to improve convective heat transfer.

SCP actuators are ideally suited for robotic applications where the muscle form factor is necessary or a boon. They offer excellent actuation speed and forces, while exhibiting compliance and damping that emulate natural muscle fibers. Furthermore, they are extremely low-cost and easy to manufacture, making them an accessible technology. We envision that the SCP actuator will find regular use in animatronics and robotic prostheses, assistive robots, soft-robotics, do-it-yourself (DIY) robots, and many other applications.

REFERENCES

[1] R. K. Josephson, "Contraction dynamics and power output of skeletal muscle." Annual review of physiology, vol. 55, pp. 527-46, Jan. 1993.

[2] G. Pratt and M. Williamson, "Series Elastic Actuators," Proc. IEEE Conf. Intelligent Robots and Systems (IROS1995), pp. 399–406, 1995.

[3] C. Chou and B. Hannaford, "Measurement and modeling of McKibben pneumatic artificial muscles," IEEE Transactions on Robotics and Automation, vol. 12, no. 1, pp. 90–102, 1996.

[4] C. S. Haines et al., "Artificial muscles from fishing line and sewing thread." Science, vol. 343, no. 6173, pp. 868–72, Feb. 2014.

[5] J. Madden et al., "Artificial Muscle Technology: Physical Principles and Naval Prospects," IEEE Journal of Oceanic Engineering, vol. 29, no. 3, pp. 706–728, Jul. 2004.

[6] W. Huang, "On the selection of shape memory alloys for actuators," Materials & Design., vol. 23, no. 1, pp. 11–19, 2002.

[7] J. Jayender, R. V. Patel, S. Nikumb, and M. Ostojic, "Modeling and Control of Shape Memory Alloy Actuators," IEEE Transactions on Control Systems Technology, vol. 16, no. 2, pp. 279–287, 2008.

[8] M. H. Elahinia and H. Ashrafiuon, "Nonlinear Control of a Shape Memory Alloy Actuated Manipulator," Journal of Vibration and Acoustics, vol. 124, no. 4, p. 566, 2002.

[9] Y. Bar-Cohen, Electroactive Polymer (EAP) Actuators as Artificial Muscles: Reality, Potential, and Challenges. SPIE Press, 2004.136.

[10] J. Leng, X. Lan, Y. Liu, and S. Du, "Shape-memory polymers and their composites: Stimulus methods and applications," Progress in Materials Science, vol. 56, no. 7, pp. 1077–1135, Sep. 2011.

[11] R. Baughman, "Conducting polymer artificial muscles," Synthetic Metals, vol. 78, no. 3, pp. 339–353, Apr. 1996.

[12] S. Seelecke and I. Muller, "Shape memory alloy actuators in smart structures: Modeling and simulation," Applied Mechanics Reviews, vol. 57, no. 1, p. 23, 2004.

[13] R. Kornbluh and R. Pelrine, "Electrostrictive polymer artificial muscle actuators," Proc. IEEE Int. Conf. on Robotics and Automation (ICRA1998), no. May, pp. 2147–2154, 1998.

[14] T. Mirfakhrai et al., "Electrochemical actuation of carbon nanotube yarns," Smart Materials and Structures, vol. 16, no. 2, pp. S243–S249, Apr. 2007.

[15] I. Rousseau, "Challenges of shape memory polymers: A review of the progress toward overcoming SMPs limitations," Polymer Engineering & Science, 2008.

[16] S. Ashley, "Artificial muscles," Scientific American, October 2003, pp. 53–59.

[17] Z. Wang et al.,"A micro-robot fish with embedded SMA wire actuated flexible biomimetic fin," Sensors and Actuators A: Physical, vol. 144, no. 2, pp. 354–360, Jun. 2008.

[18] S. Seok et al., "Meshworm: A Peristaltic Soft Robot With Antagonistic Nickel Titanium Coil Actuators," IEEE/ASME Transactions on Mechatronics, vol. 18, no. 5, pp. 1485–1497, Oct. 2013.

[19] K. J. De Laurentis and C. Mavroidis, "Mechanical design of a shape memory alloy actuated prosthetic hand." Technology and health care : official journal of the European Society for Engineering and Medicine, vol. 10, no. 2, pp. 91–106, Jan. 2002.

[20] H. M. Herr and R. D. Kornbluh, "New horizons for orthotic and prosthetic technology: artificial muscle for ambulation," vol. 5385, pp. 1–9, Jul. 2004.

[21] M. D. Lima, et al., "Electrically, chemically, and photonically powered torsional and tensile actuation of hybrid carbon nanotube yarn muscles." Science, vol. 338, no. 6109, pp. 928–32, Nov. 2012.

[22] S. M. Mirvakili et al., "Simple and strong: Twisted silver painted nylon artificial muscle actuated by Joule heating," in Proc. SPIE, vol. 9056, Mar. 2014, p. 90560I.

[23] Y.-C. Fung, Biomechanics. Springer, 1990.